

Thermal degradation, kinetic analysis, and apoptosis induction in human melanoma for oleanolic and ursolic acids

Adriana Fuliș¹ · Ionuț Ledeti¹ · Gabriela Vlase² · Titus Vlase² · Codruța Șoica¹ · Cristina Dehelean¹ · Camelia Oprean¹ · Florina Bojin³ · Lenuța-Maria Șuta¹ · Vasile Bercean⁴ · Ștefana Avram¹

Received: 23 July 2015 / Accepted: 20 September 2015 / Published online: 1 October 2015
© Akadémiai Kiadó, Budapest, Hungary 2015

Abstract This study deals with the comparative analysis of thermal degradation (including kinetic study) in dynamic air atmosphere, for two similar-structured triterpenoid acids—ursolic (URS) and oleanolic (OLE) acids. As kinetic methods, two integral methods (Kissinger–Akahira–Sunose and Flynn–Wall–Ozawa) and one differential method (Friedman) were used. The “in-depth” kinetic analysis was completed by applying the nonparametric kinetics (NPK) method, which confirmed the multiprocess degradation suggested by isoconversional methods (the observed variation in E_a vs. conversion degree). The NPK method revealed that ursolic acid is degraded solely by two parallel chemical processes, while in the case of oleanolic acid, the processes are accompanied by physical ones. The physicochemical investigation was completed with a bioactivity evaluation regarding the apoptotic process caused by the two compounds in A2058 human melanoma cell line. It was found that the similar-structured triterpenoids possess different biological effects,

OLE being antiapoptotic, while URS being strong apoptotic.

Keywords Triterpenoid acids · Kinetic study · Oleanolic · Ursolic · NPK method · Apoptosis

Introduction

Ursolic acid [(1*S*,2*R*,4*aS*,6*aR*,6*aS*,6*bR*,8*aR*,10*S*,12*aR*,14*bS*)-10-hydroxy-1,2,6*a*,6*b*,9,9,12*a*-heptamethyl-2,3,4,5,6,6*a*,7,8,8*a*,10,11,12,13,14*b*-tetradecahydro-1*H*-picene-4*a*-carboxylic acid or 3*β*-hydroxy-12-ursen-28-ic acid], known by trivial names such as malol, urson, or prunol, is present in many plants, such as *Mirabilis jalapa* (marvel of Peru) [1], peppermint, holy basil, and in large quantities in the apple peel, but as well elderberries [2]. Ursolic acid (URS) is a potent bioactive compound, acting as inhibitor for the STAT3 activation pathway in different cancer cell types [3], and also decreases the proliferation of cancer cells [4]. Recently, URS was studied for anxiolytic-like effects of in mice [5].

Oleanolic acid [(4*aS*,6*aR*,6*aS*,6*bR*,8*aR*,10*S*,12*aR*,14*bS*)-10-hydroxy-2,2,6*a*,6*b*,9,9,12*a*-heptamethyl-1,3,4,5,6,6*a*,7,8,8*a*,10,11,12,13,14*b*-tetradecahydronicene-4*a*-carboxylic acid] or known as oleanic acid is a natural triterpene distributed in numerous medicinal plants. Oleanolic acid (OLE) and its derivatives are mainly investigated for antiviral and anti-tumor properties [6], but is also known to possess antihypertensive actions [7]. Madlala et al. [7] also reported a protocol for obtaining oleanolic acid by extraction from dried flower buds of *Syzygium aromaticum*.

The structural formulas of the studied compounds are presented in Fig. 1.

Ursolic and oleanolic acids gained much attention due to the numerous studies that report the antitumor potential of

✉ Ionuț Ledeti
ionut.ledeti@umft.ro

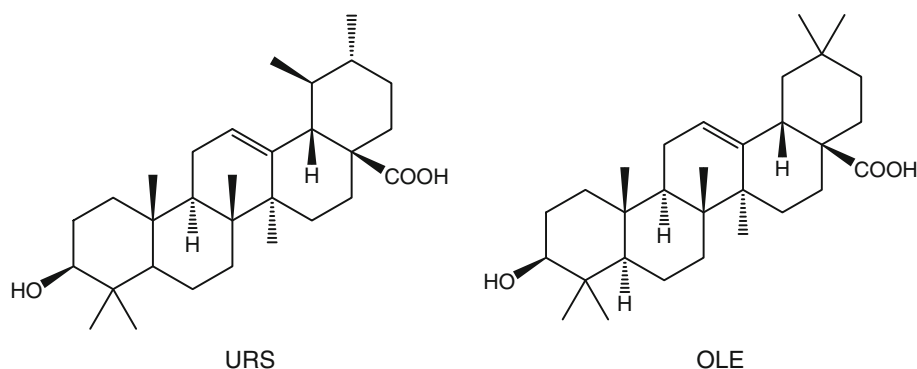
¹ Faculty of Pharmacy, “Victor Babes” University of Medicine and Pharmacy, Eftimie Murgu Square 2, 300041 Timisoara, Romania

² Research Center for Thermal Analysis in Environmental Problems, Faculty of Chemistry-Biology-Geography, West University of Timisoara, Pestalozzi Street 16, 300115 Timisoara, Romania

³ Faculty of Medicine, “Victor Babes” University of Medicine and Pharmacy, Eftimie Murgu Square 2, 300041 Timisoara, Romania

⁴ Faculty of Industrial Chemistry and Environmental Engineering, Politehnica University Timișoara, 6 Carol Telbisz, 300001 Timisoara, Romania

Fig. 1 Structural formulas of ursolic acid (URS) and oleanolic acid (OLE)



the triterpenic compounds [8–13]. Their mechanism of antitumor activity is one of the most addressed topics on research. As defective apoptosis is one of the most important factors in cancer development [14], apoptosis had become a target in cancer therapy [15].

Following some previous studies employed in our research group [16–20], this study aimed toward two main directions, namely reporting the comparative thermal degradation behavior by means of kinetic analysis over the ursolic and oleanolic acids, followed by a comparative biological activity by *in vitro* protocols. According to this, for the kinetic analysis, DTG data obtained at five heating rates ($\beta = 5, 7, 10, 12,$ and $15\text{ }^{\circ}\text{C min}^{-1}$) in air were used, for the main decomposition step of URS and OLE. As kinetic methods, Kissinger–Akahira–Sunose, Flynn–Wall–Ozawa, Friedman, and NPK were used, in accordance with ICTAC 2000 protocol. The second part of the present study assesses the role of URS and OLE in apoptosis induction in human melanoma, reporting a comparative evaluation of their *in vitro* effectiveness.

Materials and methods

Materials

Ursolic acid (URS, purity >90 %, m.p. $292\text{ }^{\circ}\text{C}$, with decomposition, U6753 Aldrich, Germany) and oleanolic acid (OLE, purity >97 %, m.p. $>300\text{ }^{\circ}\text{C}$, O5504 Aldrich, Germany) were commercial products. The compounds were used as received, without further purification and kept in sealed tubes until use, as requested by the supplier.

FTIR analysis

The FTIR spectra of samples were determined on a PerkinElmer SPECTRUM 100 device using the UATR technique. The samples were collected after 64 acquisitions, with a resolution of 4 cm^{-1} , on the spectral domain $4000\text{--}600\text{ cm}^{-1}$.

Thermal analysis and kinetic study

Thermoanalytical data TG/DTG/HF were obtained after taking measurements on a PerkinElmer DIAMOND TG/DTA instrument. The experiments were carried out using 6 mg of sample (for both URS and OLE) which was weighted into open aluminum crucibles. The temperature was programmed to increase linearly under non-isothermal conditions from $25\text{ }^{\circ}\text{C}$ up to $500\text{ }^{\circ}\text{C}$, at heating rates $\beta = 5, 7, 10, 12,$ and $15\text{ }^{\circ}\text{C min}^{-1}$. The experiments were completed in a synthetic air atmosphere at a flow rate of 100 mL min^{-1} , and the kinetic study was carried out for the main decomposition step that took place between $215\text{--}375\text{ }^{\circ}\text{C}$ (OLE) and $242\text{--}375\text{ }^{\circ}\text{C}$ (URS).

Cell culture

A2058 human melanoma cell line was purchased from ATCC, USA. Cells were cultured in DMEM (Sigma-Aldrich) containing 10 % FCS (Fetal Calf Serum, PromoCell, Heidelberg, Germany), 1 % L-glutamine (Sigma-Aldrich), and 1 % penicillin–streptomycin (Pen/Strep, 10,000 IU mL^{-1} ; PromoCell). Cells were maintained in an atmosphere of 5 % CO_2 at $37\text{ }^{\circ}\text{C}$. The cell lines were seeded onto a six-well plate (10^6 cells well^{-1}) and attached to the bottom of the well for 24 h. The next day, 2.5 mL of new medium containing the tested substances (URS and OLE) was added, and cells were incubated for 48 h. The tested concentrations were 50 and $75\text{ }\mu\text{M}$. Untreated cells were used as control. After 48 h of exposure to URS and OLE, the cells were detached from the culture flasks using 0.25 % Trypsin/0.53 mM EDTA solution (ATCC, Germany), and the apoptotic process was tested by flow cytometry.

Annexin V/PI assay

For the cell death flow cytometry studies (apoptosis), Annexin V FITC (Miltenyi Biotec, Gladbach, Germany) combined with propidium iodide staining solution (BD

Biosciences, San Jose, CA, USA) were used. 10^6 cells were washed in $1 \times$ Annexin V Binding Buffer (BD Pharmigen), centrifuged at 300 g for 10 min, suspended in the same solution, and incubated with 10 μ L of Annexin V FITC for 15 min in the dark at room temperature. The cells were washed with 1.0 mL specific binding buffer and centrifuged, and then, the cell pellet was suspended in 500 μ L binding buffer. 1.0 μ g mL^{-1} of PI solution was added immediately prior to analysis by flow cytometry. All in vitro experiments were performed on plates with three parallel wells. The results are presented as mean \pm SD. One-way ANOVA test was used to determine the statistical difference between various experimental groups; * indicate $p < 0.05$.

Results and discussion

FTIR spectroscopy

In order to confirm the purity of the analyzed samples, the FTIR spectra of both URS and OLE were drawn up and presented in Fig. 2. FTIR spectra of both compound showed similarities, since the structures are similar. The broad bands around 3500 and 3000 cm^{-1} (3672–3388 cm^{-1} , 3122–2820 cm^{-1} for OLE and 3622–3379 cm^{-1} , 3105–2819 cm^{-1} for URS) indicate the presence of hydroxyl groups in the structure, as well the presence of the C–H bonds. The intense bands at 1698 cm^{-1} for OLE and 1716 cm^{-1} for URS are due to the presence of carboxylic C=O moiety.

Thermal analysis

Oleanolic acid (OLE) exhibits one decomposition stage in the temperature range 200–350 $^{\circ}\text{C}$ with a mass loss of $\approx 99\%$. For the ursolic acid (URS), the thermoanalytical

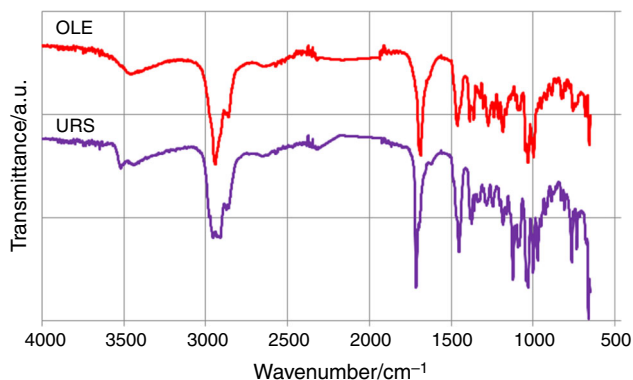


Fig. 2 UATR-FTIR spectra of the analyzed triterpenic acids—OLE and URS

behavior is similar, which indicates a comparable thermal stability. The mass loss occurs in the same temperature range, but the maximum of the DTG curve appears at 311 $^{\circ}\text{C}$ for URS, while for OLE it was at 286 $^{\circ}\text{C}$, at the same heating rate (5 $^{\circ}\text{C min}^{-1}$) (Figs. 3, 4).

In both cases, due to thermal inertia of the sample, the thermoanalytical processes appear at higher temperatures with the increase in the heating rate. However, the maximum of the degradative processes are in the temperature range 285–350 $^{\circ}\text{C}$ for OLE and 300–360 $^{\circ}\text{C}$, when the heating rate increased from 5 to 15 $^{\circ}\text{C min}^{-1}$. The HF (heat flow) curves for URS and OLE (Fig. 5) allowed determination of the melting points which are in agreement with the literature data, i.e., for OLE ($T_{\text{max HF}} = 303.8$ $^{\circ}\text{C}$) and URS ($T_{\text{max HF}} = 285.7$ $^{\circ}\text{C}$) [21, 22]. Since the thermal behavior was similar, a kinetic study was further employed.

Kinetic study

Kinetic analysis of heterogeneous degradation of bioactive compounds and potential bioactive compounds is of highly interest in pharmaceutical field, since the stability plays a key role in developing new pharmaceutical formulations. As known, before employing thermal stability over the final pharmaceutical formulation, the active pharmaceutical ingredient (API) must be completely characterized by physicochemical methods. According to this, numerous papers reported the behavior of compounds under thermal treatment [16–19, 23].

Kinetic analysis carried out for heterogeneous decomposition of APIs reveals information regarding the stability and decomposition mechanism through the values of activation energy (E_a), reaction order (n), and pre-exponential factor (A).

The first part of our study was focused on the evaluation of thermal-induced degradation of URS and OLE in air atmosphere through kinetic analysis. All the processing of the data was carried out with the use of isoconversional methods, as the ICTAC 2000 recommended. Three methods—two integral, (Flynn–Wall–Ozawa, FWO and Kissinger–Akahira–Sunose, KAS) and one differential (Friedman)—were used. The study was then completed with the use of nonparametric kinetics method (NPK), for a correct estimation of complex processes such as parallel steps in thermal destruction of molecular skeletons. The advantages of employing isoconversional methods in the analysis of heterogeneous degradation were elsewhere explained [24], and as well the theoretical aspects regarding the elaboration of NPK method [25, 26] and its modification [27, 28].

The equations describing the selected isoconversional methods of Flynn–Wall–Ozawa (FWO) [29, 30], Kissinger–Akahira–Sunose (KAS) [31, 32], and Friedman (Fr) [33], and as well the NPK method, are presented in Table 1.

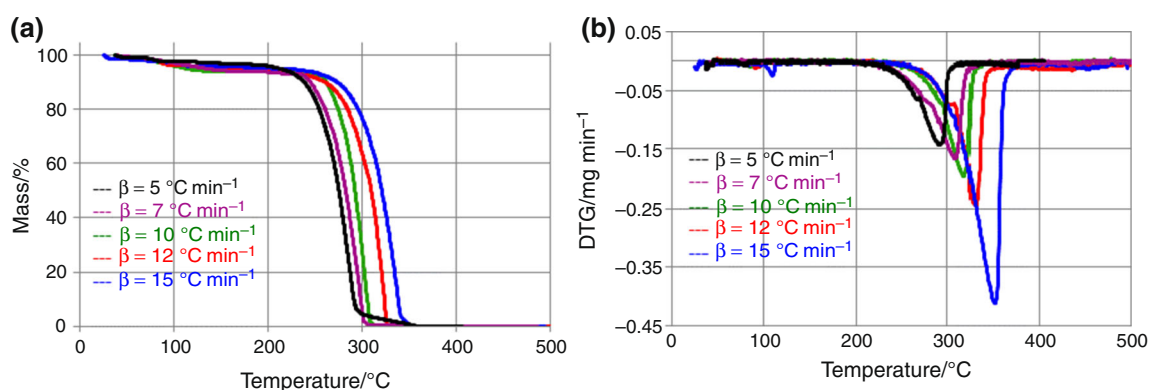


Fig. 3 Thermoanalytical curves **a** TG and **b** DTG registered at five heating rates for OLE

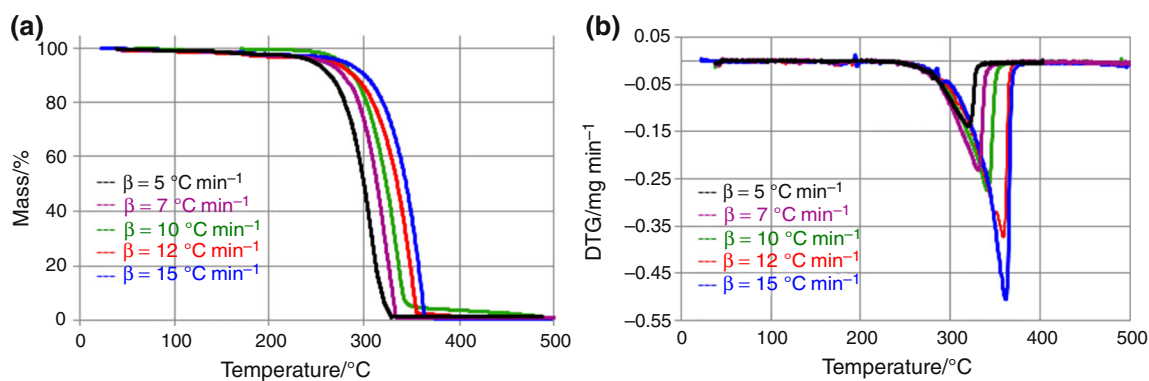


Fig. 4 Thermoanalytical curves **a** TG and **b** DTG registered at five heating rates for URS

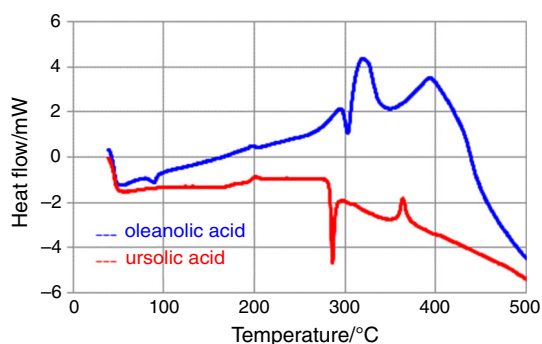


Fig. 5 HF curves for the two analyzed compounds

As abbreviations are used: α —conversion degree, T —temperature, $f(\alpha)$ —the differential conversion function, $g(\alpha)$ —the integral conversion function, R —the universal gas constant, β —the heating rate and $\beta = dT/dt$ (where t —time), $k(T)$ —a temperature dependence, A —the pre-exponential factor, and E_a —the activation energy given by the Arrhenius equation.

By plotting the data according to the methods described in Table 1, linear correlations were obtained for isoconversional methods, and the estimation of E_a values was realized

Table 1 Employed kinetic methods used to describe the thermal degradation of OLE and URS

Method	Equation	Plotting
FWO	$\ln \beta = \ln \frac{A}{R \cdot g(\alpha)} - 5.331 - \frac{1.052 \cdot E_a}{R \cdot T}$	$\ln \beta$ versus $(1/T)$
KAS	$\ln \frac{\beta}{T^2} = \ln \frac{A \cdot R}{E_a \cdot g(\alpha)} - \frac{E_a}{R \cdot T}$	$\ln (\beta/T^2)$ versus $1/T$
Fr	$\ln \left(\beta \frac{d\alpha}{dT} \right) = \ln [A \cdot f(\alpha)] - \frac{E_a}{R \cdot T}$	$\ln \left(\beta \frac{d\alpha}{dT} \right)$ versus $(1/T)$
NPK	$\frac{d\alpha}{dT} = k(T) \cdot f(\alpha)$	3D

from the slopes of those lines, for $0.05 \leq \alpha \leq 0.95$, with a α -variation step of 0.05. The linear plots are presented in Fig. 6. The obtained results are presented in Fig. 7; for each case, determination coefficients were higher than 0.974, indicating good linear correlations.

According to the three isoconversional models, a significant variation in the activation energy depending on the conversion degree was observed. Integral methods revealed a variation greater than 10 % for OLE, for lower and higher conversion degrees—from 42.8 to 74.6 kJ mol⁻¹, while for URS, only the starting of the process was outside

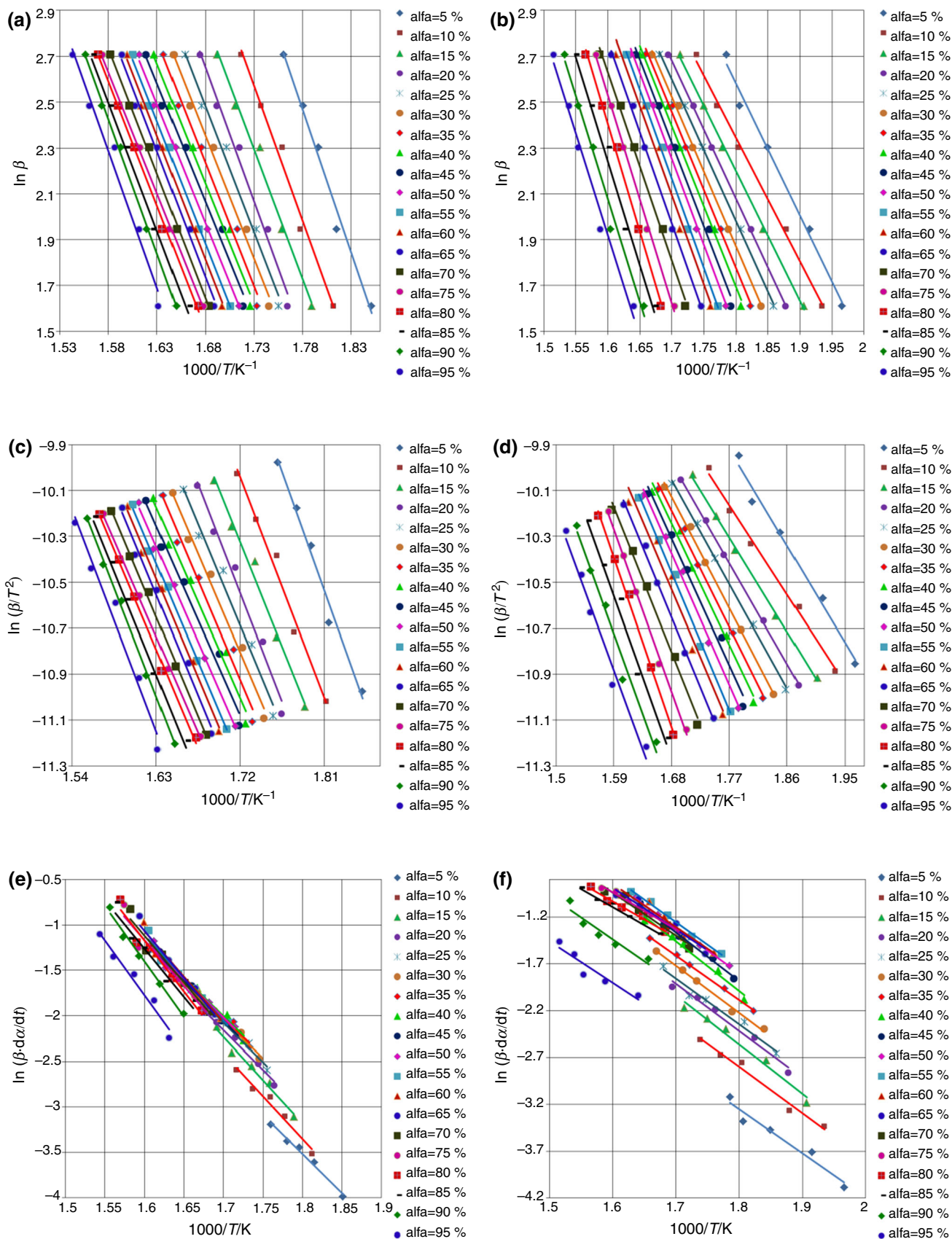


Fig. 6 Linear plots obtained for degradation of URS: **a** FWO, **c** KAS and **e** Fr and OLE; **b** FWO, **d** KAS and **f** Fr

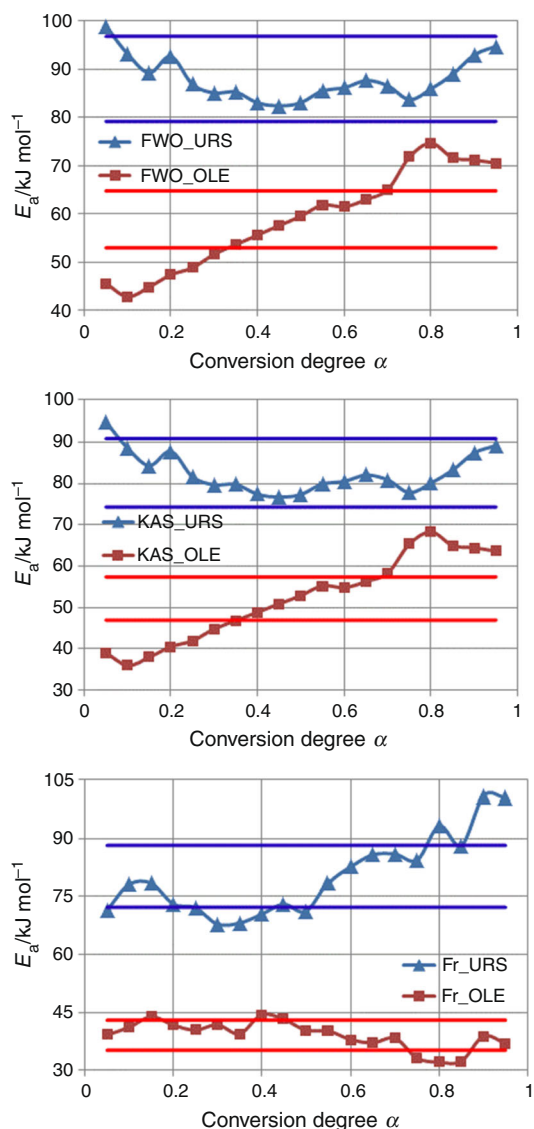


Fig. 7 Activation energy (E_a) versus α by the three applied isoconversional methods (with $\pm 10\%$ variations from the mean values which were marked with the parallel lines with O \times)

the limit. Friedman method revealed a different behavior: The variation in E_a for URS was dispersed outside the 10% limit, while for OLE, the values were much closer to the medium value.

This fact suggests that the mechanisms' decomposition is influenced by the heating rate and conversion degree, and the results suggested by the isoconversional methods must be validated and correlated with the NPK method.

The nonparametric kinetic (NPK) method is based solely on the assumption of the validity of Arrhenius equation, so that the reaction rate can be expressed as a product of two independent functions, $f(\alpha)$ and $k(T)$.

The experimental values of reaction rates are arranged in a matrix which is expressed as a product of two vectors

containing information on $k(T)$ and $f(\alpha)$. The experimental points obtained at five heating rates form by interpolation a three dimensional continuous reaction rate surface, with the following coordinates: T , α , and transformation rate (Fig. 8). By discretization, from this surface, it was obtained an $n \times m$ matrix M , which is decomposed, using the singular value decomposition algorithm [34], into the product of matrixes:

$$M = U(\text{diag } S)V^T \quad (1)$$

The results of NPK analysis are presented in Table 2. These data were obtained by analyzing the vector u (the first column of U) in respect of a kinetic model suggested by Šesták and Berggren [35]:

$$f(\alpha) = \alpha^m \cdot (1 - \alpha)^n, \quad (2)$$

respectively, the vector v (the first column of V) for an Arrhenius-type temperature dependence.

For URS, the major process with explained variance $\lambda = 70.5\%$ is only a chemical degradation with a reaction order $n = 1/3$, unaccompanied by any physical process ($m = 0$). The second process has a greater value for activation energy, but it contributes to the final energy in a smaller proportion, since $\lambda = 27.4\%$. However, this second process is only of chemical nature, but with an unitary reaction order ($n = 1$).

For OLE, the degradation process is more complex than in the case of URS, since both stages involve chemical degradation processes, associated with physical ones ($n \neq 0$ and $m \neq 0$). In each case, processes with insignificant value for explained variance ($\lambda < 10\%$) were not taken into account.

The results presented as medium values for E_a for KAS, FWO, and Fr methods in Table 2 should be taken into account solely for comparison with the ones obtained by the NPK method, and not as absolute values calculated as mean for the entire process, since it is clear that the decomposition is in both cases multistadial with different decomposition pathways.

Since the molecular structures of both URS and OLE contain the same pentacyclic triterpenoid moiety, which is in each case similarly substituted (both as means of position and volume of substituents), the great differences observed in the values of activation energies (79.2 kJ mol^{-1} for URS vs. 44.6 kJ mol^{-1} for OLE) and as well as in the mechanism of decomposition (solely chemical for URS and physicochemical for OLE) were not expected to be found.

Analyzing the values obtained by applying Friedman method, it is observed a significant variation in these values (more than 10%) with the conversion degrees. This fact can be interpreted as a multistage reaction of thermal degradation. Only one isoconversional method (FR)

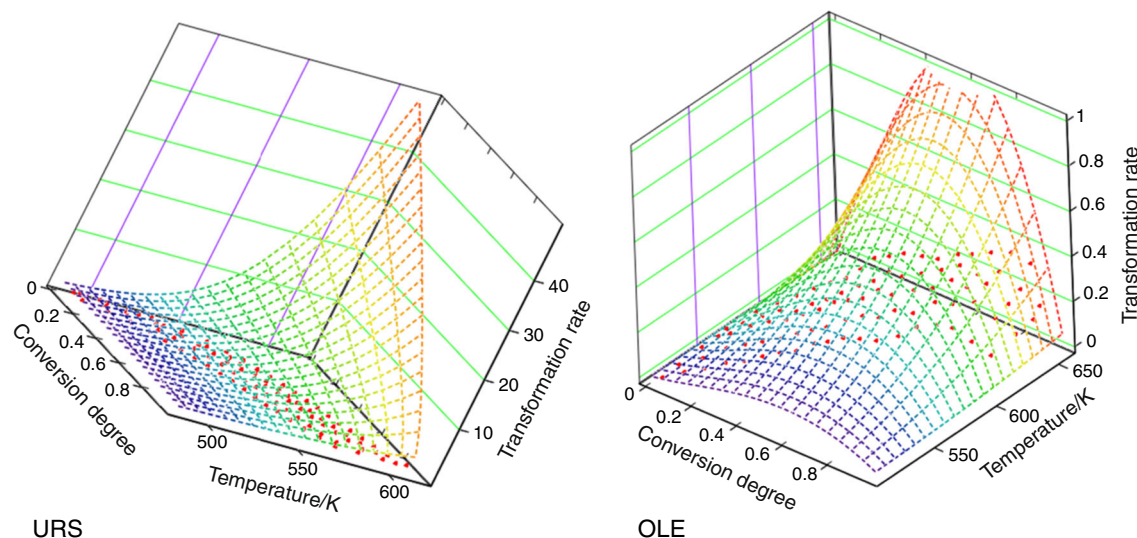


Fig. 8 3D transformation rate surfaces for URS and OLE obtained by the NPK method

Table 2 Results of the NPK method for the analysis of URS and OLE and comparison with isoconversional methods

Sample	Process	$\lambda/\%$	$E/\text{kJ mol}^{-1}$	A/s^{-1}	n	m	Šestak–Berggren eq.	$\bar{E}/\text{kJ mol}^{-1}$			
								NPK	KAS	FWO	Fr
URS	1	70.5	64.9 ± 2.3	4.925×10^6	1/3	0	$(1 - \alpha)^{1/3} \cdot \alpha^0$	79.2 ± 3.6	82.6 ± 1.1	87.9 ± 1.0	80.2 ± 2.3
	2	27.4	114.0 ± 7.4	8.217×10^{11}	1	0	$(1 - \alpha) \cdot \alpha^0$				
OLE	1	80.1	40.7 ± 2.3	1.112×10^4	1	3/2	$(1 - \alpha)^1 \cdot \alpha^{3/2}$	44.6 ± 2.7	52.2 ± 2.4	58.9 ± 2.4	39.1 ± 0.8
	2	18.8	63.8 ± 4.5	1.945×10^5	4/5	1/3	$(1 - \alpha)^{4/5} \cdot \alpha^{1/3}$				

highlighted this complexity of degradation, and it is due to the differential processing of the kinetic data and confirms the results obtained by the NPK method.

Bioactivity evaluation

The Annexin V FITC assay was performed in order to test the apoptotic process caused by URS and OLE in A2058 human melanoma cell line. URS and OLE activities were monitored 48 h after exposure to 50 and 75 μM of the tested substances. The tested concentrations were selected based on our studies that revealed an IC_{50} between 50 and 75 μM for URS (data not shown). As a comparative study, the same concentrations were used for OLE.

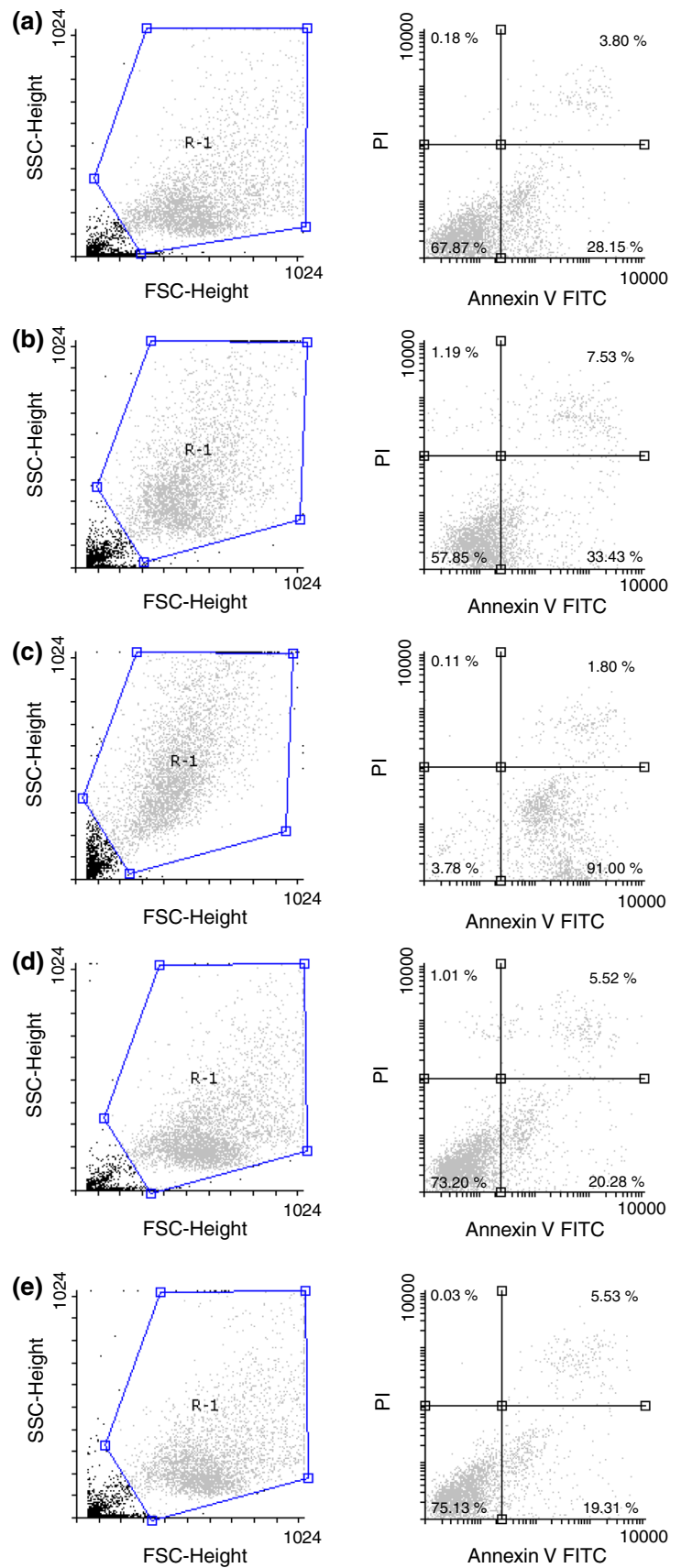
Figure 9 shows a representative A2058 melanoma cell line viability assay after 48-h URS and OLE treatment using Annexin V/PI.

As Fig. 10 shows, URS had a strong proapoptotic effect on A2058 human melanoma cells compared with the untreated cells used as control. Its apoptotic activity was in a dose-dependent manner, percentage of the early apoptotic cells being as follows: control— $28.15 \pm 2.32 \%$; URS

50 μM — $33.43 \pm 5.32 \%$; URS 75 μM — $91.00 \pm 0.04 \%$, $p = 0.04$. To the contrary, according to the Annexin V/PI staining, OLE failed to have an apoptotic effect on A2058 cells, at the same doses. Moreover, the percentage of early apoptotic cells slightly decreased after 48-h exposure to OLE compared to the untreated cells. The results are $20.28 \pm 6.50 \%$ for 50 μM of OLE and $19.31 \pm 5.37 \%$ for 75 μM , respectively, $p = 0.05$.

URS’s apoptotic activity was also reported by other groups. Wang et al. [36] reported an apoptotic activity of the compound on CAOV3 (human ovarian cancer) cell line. Shyu et al. [37] reported the role of URS in down-regulation of XIAP, the most important member of the inhibitors of apoptosis proteins (IAPs). Apoptotic activity was observed in HepG2, Hep3B, and HA22T cells (liver cancer) through the loss of MMP with the release of cytochrome *c* and other proapoptotic molecules [38]. The apoptotic effects reported by Yan et al. are for both URS and OLE. In terms of OLE, apoptotic activity was reported by Cijo-George et al. [39] on A375 (human malignant melanoma). The A375 cell apoptosis was induced at concentrations starting with 50 μM . Our results confirm the

Fig. 9 A2058 human melanoma cell line viability assay using Annexin V/PI:
a control-untreated cells,
b URS 50 μ M, **c** URS 75 μ M,
d OLE 50 μ M, and **e** OLE 75 μ M



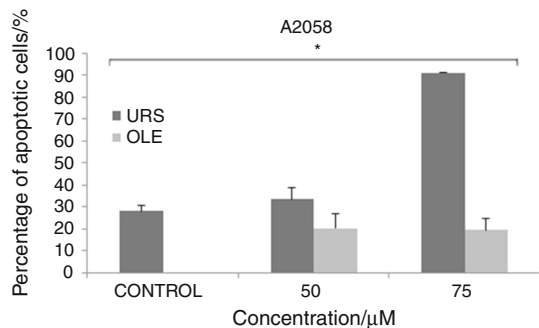


Fig. 10 Percentage of A2058 apoptotic cells after 48 h of exposure to URS and OLE (50 and 75 μM) as shown by Annexin V/PI staining

previous results in case of URS, while contrary effects were obtained for OLE. The present study reveals an antiapoptotic effect of OLE, while URS exerted a strong apoptotic activity on A2058 human melanoma cell line at the same concentrations.

Conclusions

In this study, it was reported that the results were obtained by carrying comparative thermal stability of two similar-structured pentacyclic triterpenoids, namely ursolic and oleanolic acids, which are naturally occurring bioactive compounds.

Thermal analysis revealed that URS is stable up to 242 $^{\circ}\text{C}$, while OLE is stable up to 215 $^{\circ}\text{C}$. The thermal stability was “in depth” investigated by means of kinetic analysis, in order to evaluate the kinetic triplet for this step of degradation, employing three isoconversional methods and completed by the NPK method.

The accurate determination of stability was realized by using KAS, FWO, Friedman and later completed by the nonparametric kinetics (NPK) methods, in order to separate the physical versus chemical process contribution to the heterogeneous degradation of the selected molecules. The fact that the degradation occurs in more than a singular process is also revealed by the kinetic study according to Friedman method, which indicated a complex route of degradation by the variation in E_a versus conversion degree.

Also, a bioactivity study was carried out in order to evaluate the apoptotic process caused by the two compounds in A2058 human melanoma cell line. It was found that the similar-structured triterpenoids possess different biological effects, OLE being antiapoptotic, while URS being strong apoptotic.

Acknowledgements This work was supported by a grant from the University of Medicine and Pharmacy “Victor Babeș” Timișoara (Grant III-C1-PCFI-2014/2015-03 SYNTANTITUM to AF, IL, CS, CO, LMS, and SA).

References

- Siddiqui S, Siddiqui BS, Adil Q, Begum S. Constituents of *Mirabilis jalapa*. *Fitoterapia*. 1990;61(5):471–5.
- Salvador AC, Rocha SM, Silvestre AJD. Lipophilic phytochemicals from elderberries (*Sambucus nigra* L.): influence of ripening, cultivar and season. *Ind Crops Prod*. 2015;71:15–23.
- Pathak AK, Bhutani M, Nair AS, Ahn KS, Chakraborty A, Kadara H, Guha S, Sethi G, Aggarwal BB. Ursolic acid inhibits STAT3 activation pathway leading to suppression of proliferation and chemosensitization of human multiple myeloma cells. *Mol Cancer Res*. 2007;5(9):943–55.
- Wang X, Zhang F, Yang L, Mei Y, Long H, Zhang X, Zhang J, Qimuge-Suyila, Su X. Ursolic acid inhibits proliferation and induces apoptosis of cancer cells in vitro and in vivo. *J Biomed Biotechnol*. 2011;2011:419343.
- Colla AR, Rosa JM, Cunha MP, Rodrigues AL. Anxiolytic-like effects of ursolic acid in mice. *Eur J Pharmacol*. 2015;758:171–6.
- Liu J. Pharmacology of oleanolic acid and ursolic acid. *J Ethnopharmacol*. 1995;49(2):57–68.
- Madlala HP, Van Heerden FR, Mubagwa K, Musabayane CT. Changes in renal function and oxidative status associated with the hypotensive effects of oleanolic acid and related synthetic derivatives in experimental animals. *PLoS ONE*. 2015;6:e0128192.
- Sun H, Fang WS, Wang WZ, Hu C. Structure–activity relationships of oleanane- and ursane type triterpenoids. *Bot Stud*. 2006;47:339–68.
- Prasad S, Yadav VR, Sung B, Reuter S, Kannappan R, Deorukhkar A, Diagaradjane P, Wei C, Baladandayuthapani V, Krishnan S, Guha S, Aggarwal BB. Ursolic acid inhibits growth and metastasis of human colorectal cancer in an orthotopic nude mouse model by targeting multiple cell signaling pathways: chemosensitization with capecitabine. *Clin Cancer Res*. 2012;18(8):4942–53.
- Yim EK, Lee MJ, Lee KH, Umy SJ, Park JS. Antiproliferative and antiviral mechanisms of ursolic acid and dexamethasone in cervical carcinoma cell lines. *Int J Gynecol Cancer*. 2006;16:2023–31.
- Zhao X, Liu M, Li D. Oleanolic acid suppresses the proliferation of lung carcinoma cells by miR-122/Cyclin G1/MEF2D axis. *Mol Cell Biochem*. 2015;400(1–2):1–7.
- Kartina, Piyaviriyakul S, Siripong P, Vallisuta O. HPTLC simultaneous quantification of triterpene acids for quality control of *Plantago major* L. and evaluation of their cytotoxic and antioxidant activities. *Ind Crops Prod*. 2014;60:239–46.
- Meng Q, Roubin RH, Hanrahan JR. Ethnopharmacological and bioactivity guided investigation of five TCM anticancer herbs. *J Ethnopharmacol*. 2013;148:229–38.
- Kasibhatla S, Tseng B. Apoptosis in cancer. *Carcinogenesis*. 2000;21(3):485–95.
- Ferreira C, Epping M, Kruyt F, Giaccone G. Apoptosis: target of cancer therapy. *Clin Cancer Res*. 2002;8:2024–34.
- Fulias A, Vlase G, Vlase T, Soica C, Heghes A, Craina M, Ledeti I. Comparative kinetic analysis on thermal degradation of some cephalosporins using TG and DSC data. *Chem Cent J*. 2013;7(1):70.

17. Ledeti I, Fuliş A, Vlase G, Vlase T, Doca N. Novel triazolic copper (II) complex: synthesis, thermal behaviour and kinetic study. *Rev Roum Chim.* 2013;58(4–5):441–50.
18. Ledeti I, Fuliş A, Vlase G, Vlase T, Bercean V, Doca N. Thermal behaviour and kinetic study of some triazoles as potential anti-inflammatory agents. *J Therm Anal Calorim.* 2013;114:1295–305.
19. Fuliş A, Vlase G, Grigorie C, Ledeti I, Albu P, Bilanin M, Vlase T. Thermal behaviour studies of procaine and benzocaine. Part 1. Kinetic analysis of the active substances under non-isothermal conditions. *J Therm Anal Calorim.* 2013;113(1):265–71.
20. Soica C, Danciu C, Savoiu-Balint G, Borcan F, Ambrus R, Zupko I, Bojin F, Coricovac D, Ciurlea S, Avram S, Dehelean CA, Olariu T, Matusz P. Betulinic acid in complex with a gamma-cyclodextrin derivative decreases proliferation and in vivo tumor development of non-metastatic and metastatic B164A5 cells. *Int J Mol Sci.* 2014;15(5):8235–55.
21. <http://chemicaland21.com/lifescience/uh/OLEANOLIC%20ACID.htm>. Accessed July 22, 2015.
22. <http://www.chemicaland21.com/lifescience/foco/URSOLIC%20ACID.htm>. Accessed July 22, 2015.
23. Vlase T, Vlase G, Doca N, Ilia G, Fuliş A. Coupled thermogravimetric-IR techniques and kinetic analysis by non-isothermal decomposition of Cd^{2+} and Co^{2+} vinyl-phosphonates. *J Therm Anal Calorim.* 2009;97:467–72.
24. Ledeti I, Vlase G, Vlase T, Fuliş A. Kinetic analysis of solid-state degradation of pure pravastatin versus pharmaceutical formulation. *J Therm Anal Calorim.* 2015;. doi:10.1007/s10973-015-4842-3.
25. Serra R, Nomen R, Sempere J. The non-parametric kinetics. A new method for the kinetic study of thermoanalytical data. *J Therm Anal Calorim.* 1998;52:933–43.
26. Serra R, Sempere J, Nomen R. A new method for the kinetic study of thermoanalytical data: the non-parametric kinetics method. *Thermochim Acta.* 1998;316:37–45.
27. Vlase T, Vlase G, Birta N, Doca N. Comparative results of kinetic data obtained with different methods for complex decomposition steps. *J Therm Anal Calorim.* 2007;88:631–5.
28. Anghel M, Vlase G, Bilanin M, Vlase T, Albu P, Fuliş A, Tolan I, Doca N. Comparative study on the thermal behavior of two similar triterpenes from birch. *J Therm Anal Calorim.* 2013;113(3):1379–85.
29. Ozawa T. A new method of analyzing thermogravimetric data. *Bull Chem Soc Jpn.* 1965;38:1881–6.
30. Flynn JH, Wall LA. A quick direct method for determination of activation energy from thermogravimetric data. *J Polym Sci B.* 1966;4:323–8.
31. Kissinger HE. Reaction kinetics in differential thermal analysis. *Anal Chem.* 1957;29:1702–6.
32. Akahira T, Sunose T. Joint convention of four electrical institutes. Research Report Chiba Institute of Technology. *Sci Technol.* 1971;16:22–31.
33. Friedman HL. New methods for evaluating kinetic parameters from thermal analysis data. *J Polym Sci.* 1965;6C:183–7.
34. Wall ME. Singular value decomposition and principal component analysis. In: Berrar DP, Dubitzky W, Granzow M, editors. *A practical approach to microarray data analysis.* Norwell: Kluwer; 2003. p. 91–109.
35. Šesták J, Berggren G. Study of the kinetics of the mechanism of solid-state reactions at increasing temperatures. *Thermochim Acta.* 1971;3:1–12.
36. Wang X, Li L, Wang B, Xiang J. Effects of ursolic acid on the proliferation and apoptosis of human ovarian cancer cells. *J Huazhong Univ Sci Technol.* 2009;29(6):761–4.
37. Shyu MH, Kao TC, Yen GC. Oleanolic acid and ursolic acid induce apoptosis in HuH7 human hepatocellular carcinoma cells through a mitochondrial-dependent pathway and downregulation of XIAP. *J Agric Food Chem.* 2010;58:6110–8.
38. Yan S, Huang C, Wua S, Yin M. Oleanolic acid and ursolic acid induce apoptosis in four human liver cancer cell lines. *Toxicol In Vitro.* 2010;24:842–8.
39. Cijo GV, Kumar DRN, Suresh PK, Kumar RA. Apoptosis-induced cell death due to oleanolic acid in HaCaT keratinocyte cells—a proof-of-principle approach for chemopreventive drug development. *Asian Pac J Cancer Prev.* 2012;13(5):2015–20.